Original Article

Atorvastatin Ameliorates Urografin Induced Nephropathy in the Presence of Dehydration as a Risk Factor: A Histological and Morphometric Study on a Rat Model

Amal Hassem Mohammed Fouad[1], Moheb Farid Moneer Rafla[1], Hoda Mohamed Mahmoud[1], Nagwa Ebrahim El-Nefiawy[1], Youssef Shoukry Abdel-Al[1], Ahmed Farid Al-Neklawy[1,2]

[1]Department of Anatomy and Embryology, Faculty of Medicine, Ain Shams University, Egypt.
[2]Department of Physiological Sciences, Fakeeh College for Medical Sciences, Jeddah, Kingdom of Saudi Arabia.

ABSTRACT

Introduction: In this study, the protective role of atorvastatin on urografin induced renal injury with the presence of dehydration as a risk factor was assessed.

Material and Methods: Forty two male adult albino rats were randomly divided into seven groups (6 rats / group). Group I (control), group II (atorvastatin), group III (dehydration), group IV (urografin), group V (dehydration with urografin), group VI (atorvastatin pretreatment), and group VII (recovery). At the end of the experiment for each group, blood samples were collected for estimation of serum level of interleukin-6 and creatinine. After sacrifice, kidneys were extracted and processed for light and transmission electron microscopy.

Results: Examination of kidney sections from both group III and group IV showed an apparent increase in the radius of proximal and distal convoluted tubules. Also hyaline casts, vacuolated tubular cells, and vascular congestion were seen. Moreover, there was increase in serum levels of both interleukin-6 and creatinine. All these findings were found in group V. In addition, there was an apparent increase in the number of pyknotic nuclei of tubular cells per field. There was an increase in thickness of the glomerular basement membrane and irregular foot processes of podocytes. All these findings were ameliorated by administration of atorvastatin in group VI. In group VII, some features of renal damage were noticed indicating the failure of complete recovery. The morphometric results and statistical analysis confirmed the histological findings.

Conclusion: It was concluded that atorvastatin protected the kidney from urografin induced injury in the presence of dehydration as a risk factor.

Received: 24 December 2019, **Accepted:** 8 January 2020

Key Words: Atorvastatin, dehydration, protective role of atorvastatin, rat, urografin induced renal injury.

Corresponding Author: Ahmed Farid Al-Neklawy, MD, Department of Anatomy and Embryology, Faculty of Medicine, Ain Shams University, Egypt. **Tel.:** 00201001850336, **E-mail:** dr_ahmed_farid@med.asu.edu.eg

The Egyptian Journal of Anatomy, ISSN: 0013-2446, Vol. 43 No. 2

INTRODUCTION

Contrast medium induced nephropathy (CIN) is a leading cause of hospital acquired acute renal failure. There is no internationally accepted method for protection from CIN, except for extracellular fluid expansion[1, 2].

CIN was known as an acute deterioration of the kidney functions after contrast media administration in the absence of other etiologies[2, 3].

The pathophysiology of CIN is not well known. Some studies have suggested a toxic effect of the contrast medium on the renal tubules[2, 4]. In addition to its direct injury to the renal tubular epithelium, contrast medium can be taken up into the cells and impair the function of mitochondria leading to increased generation of reactive oxygen species with resultant cell death[2, 5, 6].

Contrast medium-induced nephropathy in animal models is thought to be caused by the effects of contrast media on the action of different

DOI: 10.21608/EJANA.2020.21238.1056

substances, including adenosine, dopamine-1, nitric oxide, angiotensin-II, and endothelin[7]. Other mechanisms suggested that CIN is the result of decreased production of nitric oxide due to direct endothelial damage[6].

On the basis of the pharmacologic and chemical properties, radiographic contrast agents can be classified into nonionic or ionic. These can have either a high osmolality or low osmolality. Urografin dye (Diatrizoate) is considered a high-osmolality contrast agent and is widely used in Egypt due to its low cost compared with ultravist (iopromide) which is expensive and not popular in Egypt. The osmolality of the contrast media plays an important role concerning the kidney damage. The use of low osmolality contrast media substantially decreases the risk of nephropathy in high-risk patients when compared with the use of high osmolality contrast media[8].

Statins are widely used drugs as they have cholesterol-lowering effect and cholesterol-independent effects, such as improving endothelial function as well as decreasing inflammation and oxidative stress[9]. Statins were reported to protect the kidney against IgA nephropathy and experimental nephritis in clinical practice through restoring the balance between apoptosis and proliferation in different types of renal cells[10].

In the daily practice, use of diagnostic tools in medicine increased as angiography and computed tomography with the contrast dye. But when needed in patients having a risk factor as diabetic kidney disease, the risk of mortality and morbidity was found to be higher.

Some researches focused on the protective role of many substances like beta-blockers against contrast induced kidney damage. However, reviewing the literature there have been few studies evaluating the possible protective effect of high dose atorvastatin on high osmolality contrast media (urografin) induced nephropathy. So, the aim of this study was to assess the possible protective role of high dose atorvastatin on urografin induced nephropathy in male adult albino rats in the presence of dehydration as a risk factor. Our specific objectives included the detection of histopathological findings related to nephropathy, biochemical study for kidney function, measurement of serum inflammatory markers, and histomorphometric measurements of renal structures before and after treatment.

MATERIAL AND METHODS

Animals

Forty two healthy male adult albino rats (weighing 200-250 gm) were used. The rats were locally bred at the animal house of Research Center, Ain Shams University College of Medicine, Egypt. They were housed in a suitable environment, in conventional wire-mesh cages, 3 rats /cage. They had free access to food (rat chaw) and water (ad libitum). All animals were exposed to 12 hours light-dark cycle, good ventilation, suitable temperature 22˚-25˚ c and humidity 45-50%.

Experimental design:

The animals were randomly divided into seven groups (6 rats / group):

Group I (control group): Rats were left with no intervention. Three rats were sacrificed with group VI and the other 3 were sacrificed with group VII.

Group II (atorvastatin group): Rats were given high doses of atorvastatin 30 mg/kg b.w/ day dissolved in water through oral gavage for 5 days[11] without dehydration and were sacrificed on the 6th day.

Group III (dehydration group): Rats were given unlimited access to standard rat chow but were deprived of water for three successive days[12] and were sacrificed on the 4th day.

Group IV (urografin group): A single dose 6 ml/kg b.w. of ionic high-osmolar contrast medium, meglumine/sodium diatrizoate (Urografin 76%, Berlimed S.A., Spain) was administered intravenously into the tail vein in healthy rats without dehydration[12]. Then, rats were sacrificed on the 2nd day.

Group V (dehydration with urografin group): Rats were given unlimited access to standard rat chow but were deprived of water for three successive days. Then at the 4th day ionic high-osmolar contrast medium, meglumine/ sodium diatrizoate (Urografin 76%, Berlimed S.A., Spain) was administered as in group IV. Then, rats were sacrificed on the 5th day.

Group VI (high dose atorvastatin pretreatment): Rats were given atorvastatin as in group II (for 5 days). At the 3rd day rats were deprived of water for three successive days. Rats were given unlimited access to standard rat chow. At the 6th day ionic high-osmolar contrast medium, meglumine/sodium diatrizoate (Urografin 76%, Berlimed S.A., Spain) was administered as in group IV. Then, rats were sacrificed on the 7th day.

Group VII (recovery group): Rats were given unlimited access to standard rat chow but were deprived of water for three successive days. Then at the 4th day ionic high-osmolar contrast medium, meglumine/sodium diatrizoate (Urografin 76%, Berlimed S.A., Spain) at a dose of 6 ml/kg b.w. was administered once intravenously into the tail vein[12]. Then rats were left for 2 weeks with free water and chow intake without any interventions before sacrifice and dissection.

Drugs:

Atorvastatin: was purchased from Epico Company (Cairo, Egypt). The drug was provided in 10 mg tablets which were dissolved in water.

Ionic high osmolar Urografin dye (meglumine/sodium diatrizoate) (Urografin 76%, Berlimed S.A., Spain): was purchased from Bayer company (Cairo, Egypt).

Specimens and blood samples collection:

At the end of the experiment for each group, blood samples were collected from the rats of all groups by retro-orbital method into sterile test tubes and allowed to clot for estimation of serum level of interleukin-6 (IL-6) and creatinine (Cr). At the end of the experiment, the rats were sacrificed by cervical decapitation after inhalation anesthesia. The abdominal viscera were explored and the kidneys were extracted and cut longitudinally into two equal halves. One half was placed in 10% neutral formalin for paraffin blocks processing[13], while the other half was immediately placed in 2.5 % glutaraldehyde and 4% formaldehyde for transmission electron microscopic processing[14].

Disposal of animal remains was done according to the regulation of the animal house of Medical Research Center, Ain Shams University College of Medicine, Egypt.

Histological study:

Kidney specimens were prepared for paraffin blocks for histological studies. Hematoxylin and eosin (H&E) staining was applied[15]. Semi-thin sections were prepared and stained with 1% toluidine blue[16]. All H&E and toluidine blue stained sections were examined by light microscope. Also, ultrathin sections were obtained and examined with PEM-100 transmission electron microscopy at EM unit in Ain shams University College of Science, Egypt. Electron micrographs were photographed from selected areas[14].

Image analysis and statistics:

Six randomly chosen fields from six different H & E stained sections of six different rats were examined in each group using digital photomicrographs (X 400) for measuring the radius of the convoluted tubules, number of pyknotic nuclei in tubular cells per field, the area percentage of microscopic field for extravasated red blood cells. The thickness of the glomerular filtration membrane was measured in electron micrographs (X 4000). The TS view analysis software in the Anatomy Department; Ain Shams University College of Medicine was employed. The mean values and standard deviation (SD) were calculated using SPSS statistical program version 17 (IBM Corporation, New York, USA). Analysis of variance (one way ANOVA) followed by post hoc test was performed to compare between the studied groups. With regard to probability, a *P value* less than *0.05* was considered significant and those < 0.001 were considered highly significant. Image analysis was performed by an examiner who does not know the coding of the study groups to avoid bias.

RESULTS

1. Histological results:

Group I and II (control and atorvastatin groups):

Examination of different stained sections of the atorvastatin group revealed similar findings as compared to the control group. Examination of the renal sections of rats from the control group showed that the parenchyma was formed of outer cortex and inner medulla. The medulla was divided into an outer and an inner part (Fig. 1)

The cortex demonstrated renal corpuscles, proximal convoluted tubules, loop of Henle and distal convoluted tubules. They were all separated by narrow interstitial spaces containing numerous blood vessels. The renal corpuscles were formed of tufted glomeruli enclosed by double layer of Bowman's capsule with Bowman's space in between. The glomeruli consisted of numerous capillary loops with endothelial cells and regular smooth basement membrane. The visceral layer of Bowman's capsule with podocytes was seen surrounding the capillary loops. The parietal layer was lined by simple squamous epithelium (Fig. 2).

Ultrathin sections of renal specimens of control group showed the capillary loops of the glomerulus with the lining endothelial cells, smooth regular basement membrane of uni-layer thickness, and foot processes of the podocytes adherent to the outer surface of the basement membrane. Foot processes were smooth regular and well aligned and were separated by tiny spaces that represent the filtration slits. The three components represent the filtration membrane. Mesangial cells were present between the capillaries, embedded in mesangial matrix and supported the entire glomerular tuft (Figs. 3-5).

The proximal convoluted tubules (PCT) stained sections demonstrated their lining with simple cuboidal epithelium with acidophilic cytoplasm, basally situated nuclei and prominent nucleoli. Their lumen appeared filled due to the brush border. The cytoplasm of the cells showed basal striations and numerous dark stained cytoplasmic granules. The tubules were separated by narrow interstitial spaces that contained numerous blood vessels and fibroblasts (Figs. 6,7).

EM examination of PCT revealed that the cytoplasm of the lining cells was containing dark dense bodies which resemble lysosomes, many apical vacuoles, and numerous mitochondria. The apical surface of the cells showed numerous thin microvilli projecting into the lumen and formed the brush border. The cells rested on a regular basement membrane (Fig. 8).

The distal convoluted tubules (DCT) were lined by simple cuboidal epithelium with apically situated nuclei and lightly stained cytoplasm. They have wider empty lumen compared with the PCT (Fig. 6).

EM examination of the distal convoluted tubules demonstrated the ultra-structure of their lining epithelial cells. The cytoplasm showed lysosomes, vacuoles and mitochondria in a few number compared with the PCT. The luminal border of the cell showed short sporadic microvilli projecting into the lumen in contrast to the PCT. Adjacent cells showed tight junctions (Fig. 9).

Group III (dehydration group)

Examination of different stained renal sections showed obvious alteration of the structure with particular tubular damage. Numerous cytoplasmic vacuolations of tubular cells, necrosis and shedding of the lining epithelium at some tubules were observed. Other tubules were dilated with apparent flattening of the lining cells. Widening of the interstitial spaces, hypocellular glomeruli with widening of the Bowman's space were also noted (Fig. 10).

The lumen of some PCT was occupied with homogenous acidophilic material (hyaline casts). The interstitial spaces were apparently widened compared with the control. Wide congested venous capillaries were also observed around the tubules with extravasation of red blood cells (Figs. 10 & 11).

Group IV (urografin group):

Examination of different stained sections showed manifest tubular damage. Glomeruli showed distortion of Bowman's capsule outline. Convoluted tubules demonstrated numerous cytoplasmic vacuolations or necrosis of the lining cells with pyknotic nuclei. Some tubules revealed deposition of homogenous material filling the lumen (casts). The interstitial spaces showed extravasation of red blood cells and severe infiltration with mononuclear cells (Figs. 12-14).

Group V (dehydration with urografin group):

Examination of stained renal cortical sections showed an apparent severe glomerular and a tubular structural alteration. Some glomeruli revealed distorted outlines with an irregular parietal layer of Bowman's capsule or loss of its continuity. The capillary loops appeared congested with extravasation of red blood cells or exudate into Bowman's space. Congested

blood vessels and inflammatory cell infiltrate in widened interstitial spaces were also seen (Figs. 15 & 16).

EM examination of renal corpuscles of this group showed apparent thickening of the glomerular basement membrane at many areas. The foot processes of the podocytes (visceral layer of Bowman's capsule) appeared irregular, distorted, and not well aligned at many areas (Figs. 17 & 18).

The convoluted tubules revealed obvious loss of their outlines. Some tubules showed pyknotic nuclei and necrosis of their lining epithelium. Homogenous material deposition (cast) was seen filling the lumen of some tubules. Red blood cells, exudate, mononuclear cell infiltrate were seen occupying the wide interstitial spaces between the tubules (Fig. 19).

EM examination showed distorted outline of PCT. There was apparent loss of the brush border microvilli. The mitochondria appeared fused with loss of striated appearance. The nuclear membrane showed many irregularities (Fig. 20). The DCT showed casts filling the lumen and shrinkage of nuclei of some cells (Fig. 21).

Group VI (atorvastatin pretreatment group):

Examination of the different stained renal sections revealed an apparently normal structure comparable to that of the control group. The renal cortex showed glomeruli with irregular wall in some capillary loops (Figs. 22 & 23).

EM examination demonstrated the normal architecture of renal corpuscles. The majority of capillary loops showed regular, smooth basement membrane of uniform thickness. Foot processes of podocytes appeared regular and well aligned (Figs. 24 & 25).

PCT and DCT showed an apparently normal structure except for few cytoplasmic vacuolations. Only few PCT demonstrated a partial loss of the brush border (Figs. 26 - 29).

Group VII (recovery group):

Examination of the different stained renal sections of the rats from this group revealed the presence of focal structural alterations affecting different components of the parenchyma. The cortex demonstrated some shrunken and damaged glomeruli (Fig. 30). EM examination showed an apparent increase in thickness of the glomerular capillary basement membrane at some areas. Foot processes of the podocytes appeared distorted or fused at other areas (Fig. 31).

The tubules in the outer cortical areas showed severe cytoplasmic vacuolations. The interstitial spaces demonstrated multiple, wide, and markedly congested blood vessels (Fig. 32). Some areas of the interstitium showed deposition of acidophilic homogenous hyaline material (Fig. 33), others revealed heavy inflammatory cell infiltrate (Fig. 34).

Light microscopic examination of the PCT showed a vacuolated cytoplasm of the lining cells or their detachment from the basement membrane, partial loss of brush border, and an apparent increase in the thickness of basement membrane. Some tubules showed homogenous material deposition filling the lumen (Fig. 35). EM examination of some areas showed nuclear membrane irregularity, partial loss of the brush border, few number of mitochondria that appeared distorted with loss of striated appearance; numerous large vacuolations occupied the basal and apical part of the cytoplasm, and apparently thick basement membrane of the lining cells (Fig. 36).

Light microscopic examination of the DCT revealed flattening of the lining epithelial cells, cytoplasmic vacuolations, and necrotic sloughed detached cells at some tubules (Fig. 37). EM examination showed detached brush border microvilli, shrunken nuclei, and loss of histological architecture of cytoplasmic organelles (Fig. 38).

2. Morphometric results and statistics:

A morphometric study was conducted and statistically analyzed. No significant differences were noted in the atorvastatin group (group II) in comparison with the control group (group I).

Radius of the PCT: (Table 1) and (Histogram 1)

Analysis of the radius of the PCT in different groups showed that there was a significant increase in dehydration group (group III) in comparison

with the control group (group I). Furthermore, there was a high significant increase in the radius of the PCT in dehydration with urografin group (group V) and recovery group (group VII) as compared with the control group (group I).

In the atorvastatin pretreatment group (group VI), the radius of the PCT recorded a highly significant decrease as compared with the dehydration with urografin group (group V). In the recovery group (group VII), there was non-significant decrease in comparison to dehydration with urografin group (group V).

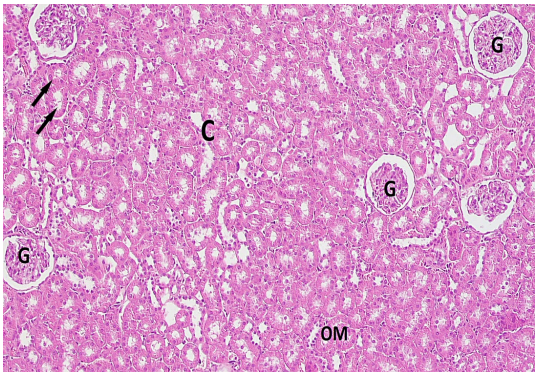

Fig. 1: A photomicrograph of a section of a control rat's kidney group (group I) showing cortex (C) containing glomeruli (G), convoluted tubules (arrows) and outer medulla (OM). (H & E, x100)

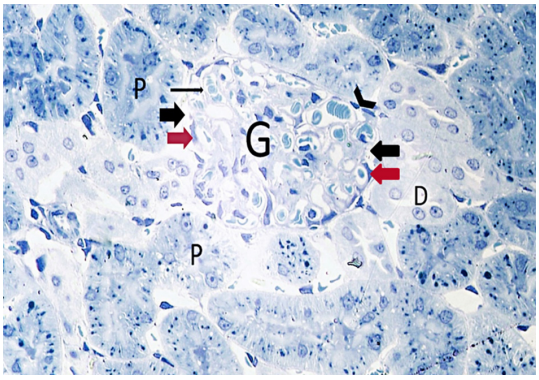

Fig. 2: A photomicrograph of a semithin section of a control rat's kidney (group I) showing glomerulus (G) with many capillaries, podocyte of visceral layer of the Bowman's capsule (red arrow), regular smooth basement membrane of the capillaries is also visible (thin arrow). The glomerulus is surrounded by distinct Bowman's space (thick black arrow). The parietal layer of Bowman's capsule is lined by simple squamous epithelium (arrow head). Notice the PCT (P) with their characteristic darkly stained lining cells with many granules and DCT with their lightly stained lining cells (D). (Toluidine blue, x400)

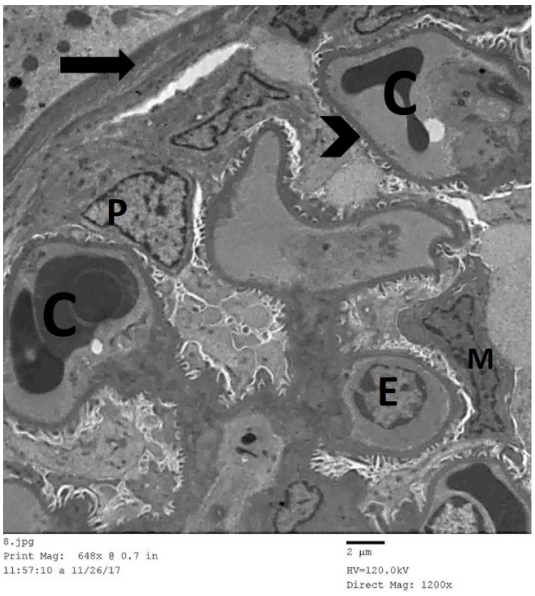

Fig. 3: An electron micrograph of an ultrathin section of a control rat's kidney (group I) showing part of a renal corpuscle. Notice Bowman's capsule parietal layer (arrow), blood capillaries with red blood cells (C), podocyte cell (P), endothelial cell (E). Mesangial cell (M) is located between and outside blood capillaries and appears irregular in outline with its processes extending towards the glomerular filtration membrane. Well defined regular basement membrane of the glomerular capillaries can be seen (arrow head). (Uranyl acetate and lead citrate, x1200)

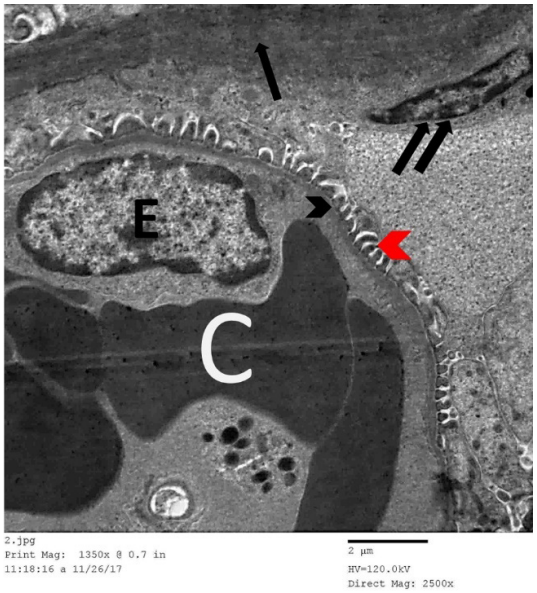

Fig. 4: An electron micrograph of an ultrathin section of a control rat's kidney (group I) showing part of a renal corpuscle. The parietal layer of Bowman's capsule (arrow) is lined by simple squamous epithelium (double arrow). A glomerular capillary is seen (C) containing red blood cells and is lined with endothelial cell (E). Well defined regular basement membrane lies exterior to glomerular endothelium (black arrow head). Podocytes foot processes can be seen exterior to capillary basement membrane (red arrow head) and are separated from each other by filtration slits. (Uranyl acetate and lead citrate, x2500)

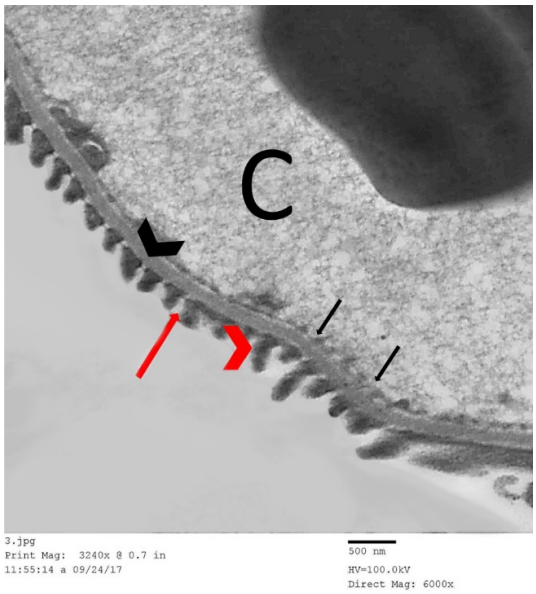

Fig. 5: An electron micrograph of an ultrathin section of a control rat's kidney (group I) showing a glomerulus loop (C) with well-defined regular smooth basement membrane (arrow head). Foot processes (red arrow head) of the podocyte are seen touching the basement membrane externally and leaving filtration slits in between (red thin arrow). Pores of the endothelial lining (black arrows) are visible. (Uranyl acetate and lead citrate, x2500)

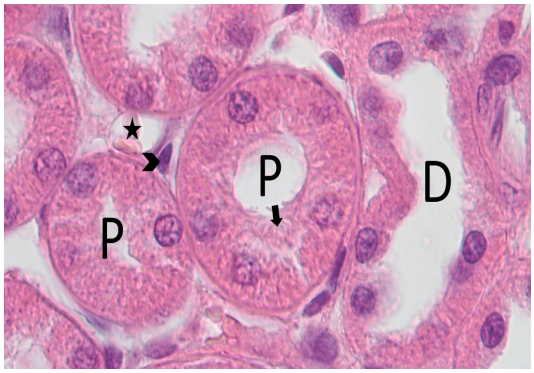

Fig. 6: A photomicrograph of a section of a control rat's kidney (group I). The proximal convoluted tubules (P) are lined by simple cuboidal epithelium with basally situated nuclei and acidophilic cytoplasm. Their lumen appeared filled due to the brush border (arrow). The distal convoluted tubule (D) is lined by simple cuboidal epithelium with apically situated nuclei and lightly stained cytoplasm. They have wider empty lumen. Peritubular capillaries can be observed (star). Fibroblast interstitial cells of the cortex are noted (arrow head). (H&E, x1000)

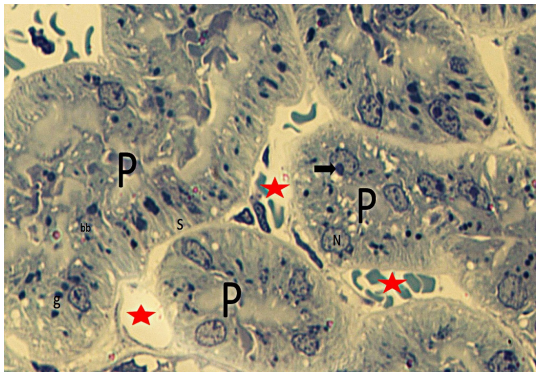

Fig. 7: A photomicrograph of a semithin section of a control rat's kidney (group I). The proximal convoluted tubules (P) are lined by simple cuboidal epithelium with a narrow lumen, basally situated nuclei (N), prominent nucleolus (arrow), brush border (bb), basal striations (s) and cytoplasmic granules (g). Notice abundant peritubular capillaries lined by simple squamous epithelium (stars). (Toluidine blue, x1000)

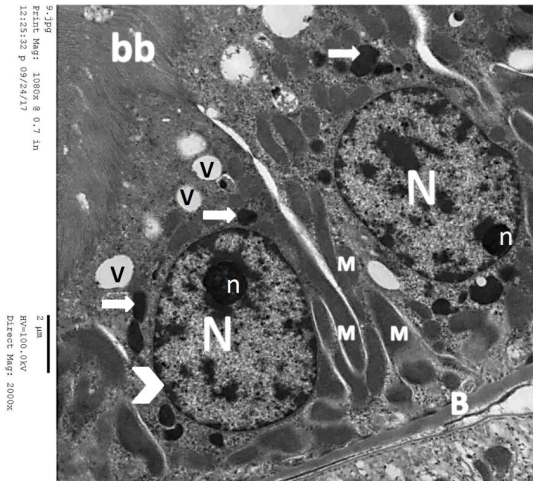

Fig. 8: An electron micrograph of an ultrathin section of a control rat's kidney (group I) showing two cuboidal cells lining the proximal convoluted tubule (PCT). The cells have basally situated rounded nuclei (N), prominent nucleoli (n), smooth nuclear membrane (arrow head), cytoplasm with dark dense bodies which resemble lysosomes (arrows), numerous mitochondria (M), many apical vacuoles (V), apical brush border (bb) made up of long numerous microvilli, and basement membrane (B). (Uranyl acetate and lead citrate, x2000)

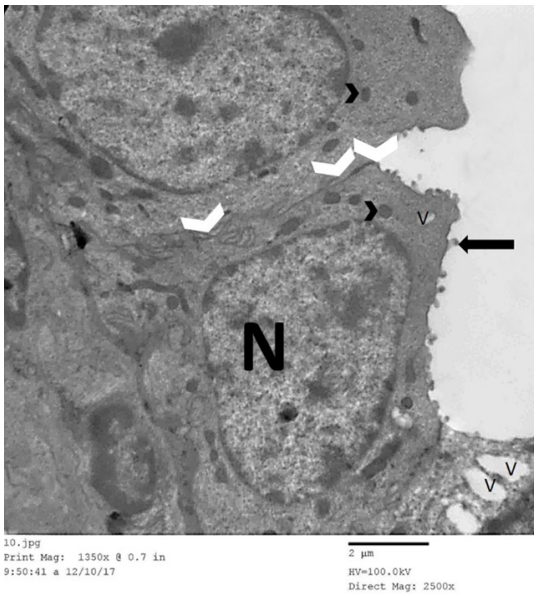

Fig. 9: An electron micrograph of an ultrathin section of a control rat's kidney (group I) showing lining epithelial cells of a distal convoluted tubule. The cytoplasm demonstrates lysosomes (black arrow heads), and vacuoles (V). The luminal border of the cell shows short sporadic microvilli projecting into the lumen (black arrow). Tight junction can be observed between adjacent lining cells (white arrow heads). (Uranyl acetate and lead citrate, x2500)

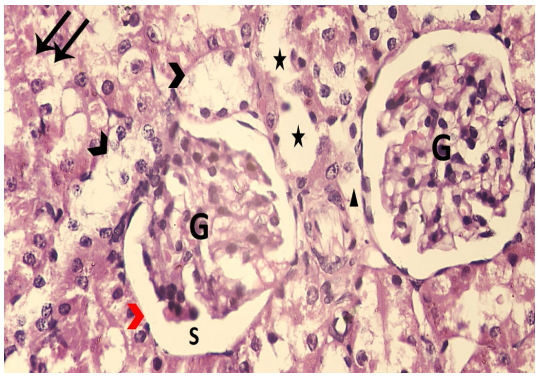

Fig. 10: A photomicrograph of a section of a rat's kidney from the dehydration group (group III) showing numerous cytoplasmic vacuolations of lining tubular cells (double arrows), necrosis and shedding of the lining epithelium at some tubules (black arrow head). Other tubules are dilated with apparent flattening of the lining cells (stars). Note the hypocellular glomeruli (G) with widening of the Bowman's space (S). (Red arrow head) = parietal layer of Bowman's capsule. (H&E, x400)

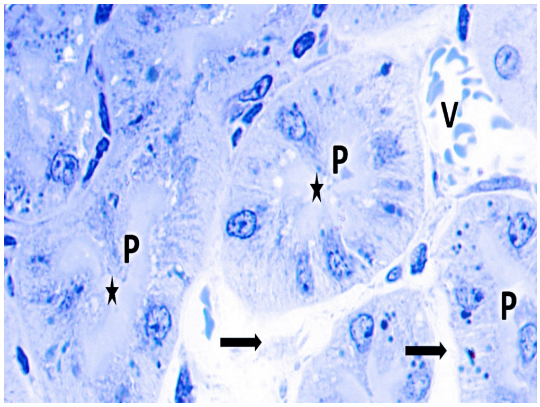

Fig. 11: A photomicrograph of a semithin section of a rat's kidney from the dehydration group cortex (group III) showing proximal convoluted tubules (P) with their lumen filled with homogenous material (stars). The interstitial spaces are apparently widened (arrows). Also wide congested venous capillaries are observed around the tubules (V). (Toluidine blue, x1000)

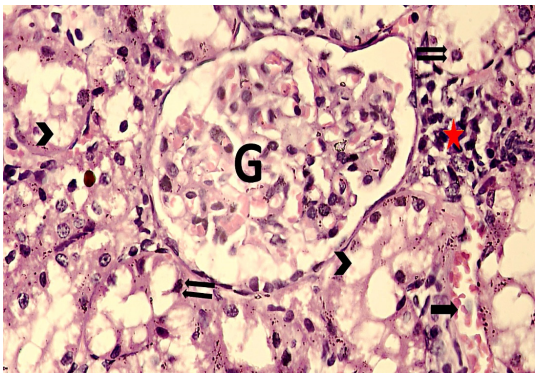

Fig. 12: A photomicrograph of a section of a rat's renal cortex from the urografin group (group IV) showing extensive vacuolation of the tubular lining epithelium (arrow head). Other tubules demonstrate pyknotic nuclei and necrosis of the lining epithelium (double arrows). Interstitial hemorrhage (arrow) and severe mononuclear cell infiltration (star) are also seen. (G) = glomerulus. (H&E, x400)

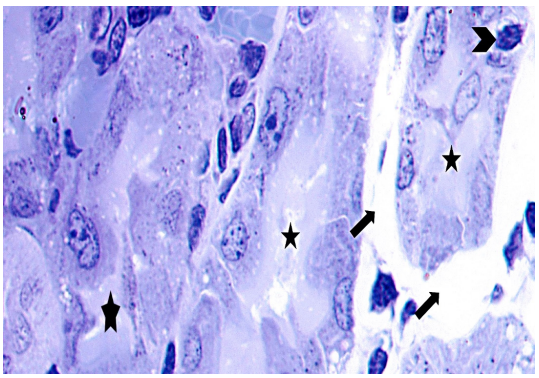

Fig. 13: A photomicrograph of a semithin section of a rat's renal cortex from the urografin group (group IV) showing deposition of homogenous material (stars) in the widened tubular lumen and pyknotic nucleus of the lining epithelium (arrow head). Notice widening of the interstitial space between the tubules (black arrows) with mononuclear cell infiltrate.(Toluidine blue, x1000)

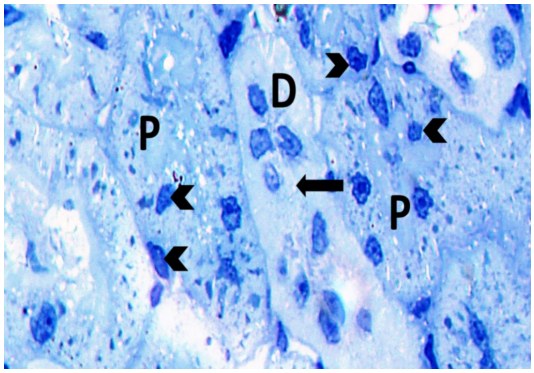

Fig. 14: A photomicrograph of a semithin section of a rat's renal cortex from the urografin group (group IV) showing severely damaged proximal convoluted tubules (P) and distal convoluted tubules (D) as most of nuclei of the lining epithelium demonstrate pyknotic changes (arrow heads). The lumen of distal convoluted tubules (D) is totally occluded (black arrow) with loss of architecture of the lining epithelium. (Toluidine blue, x1000)

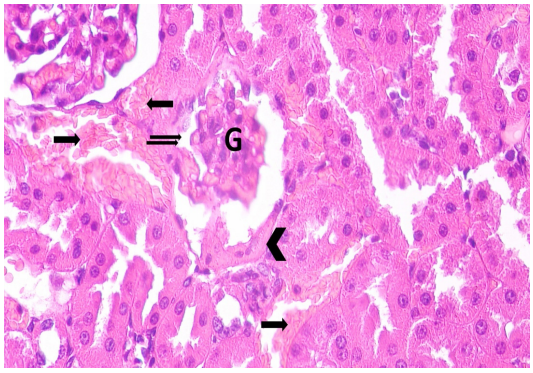

Fig. 15: A photomicrograph of a section of a rat's renal cortex from the dehydration with urografin group (group V) showing loss of continuity (double arrows) of the parietal layer of Bowman's capsule of a glomerulus (G), adherence with glomerular wall at some sites (arrow head). Notice the severe interstitial vascular congestion (single black arrows). (H&E, x400)

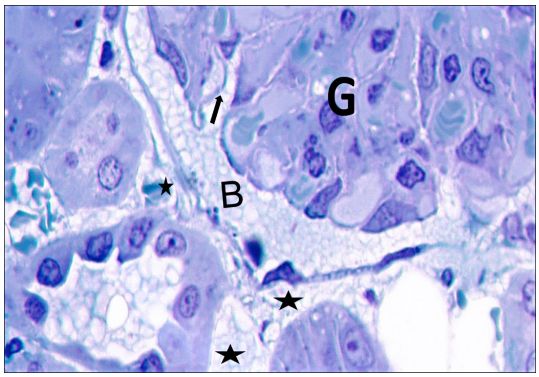

Fig. 16: A photomicrograph of a semithin section of a rat's kidney cortex from the dehydration with urografin group (group V) showing glomerulus (G) with thickened glomerular basement membrane (black arrow). Both Bowman's space (B) and the interstitial spaces (stars) are widened and filled with exudate. (Toluidine blue, x1000)

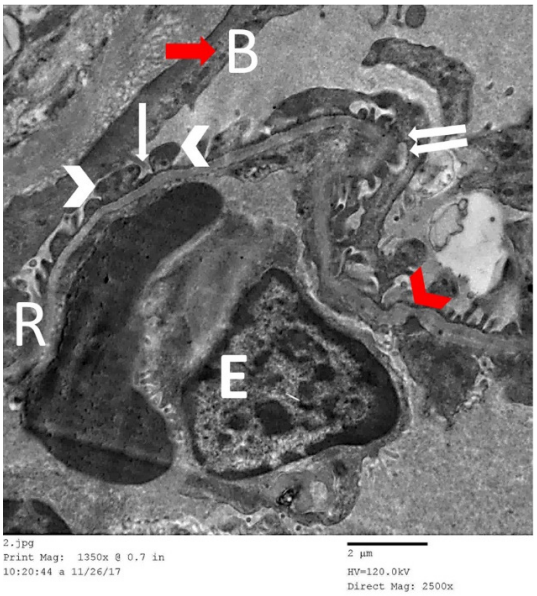

Fig. 17: An electron micrograph of an ultrathin section of a rat's kidney cortex from the dehydration with urografin group (group V) showing part of a renal corpuscle that reveals parietal layer of Bowman's capsule (red arrow), Bowman's space (B), part of a capillary lumen with red blood cells (R) ,and lining endothelial cell (E). Notice thickening of the glomerular basement membrane at some sites (red arrow head). Note the foot processes (white arrow heads) of podocytes adherent to the outer surface of glomerular capillary membrane leaving filtration slits in between (white arrow), and looks markedly distorted at some sites (double white arrows). (Uranyl acetate and lead citrate, x2500)

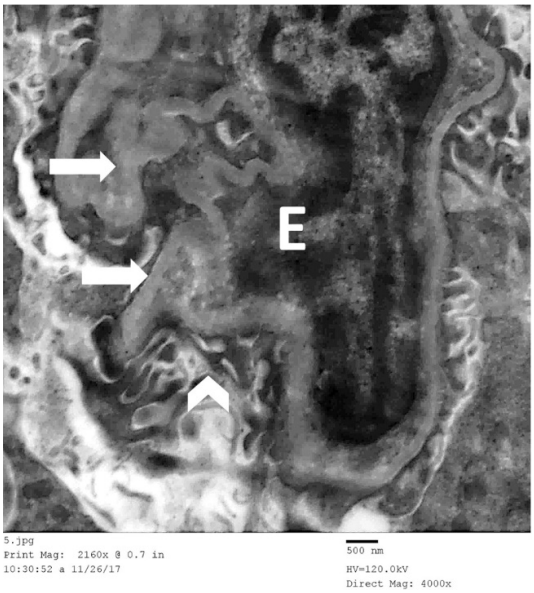

Fig. 18: An electron micrograph of an ultrathin section of a rat's kidney cortex from the dehydration with urografin group (group v) showing part of a renal corpuscle that reveals capillary lumen with lining endothelial cell (E). Notice thickening of the glomerular filtration membrane at some sites (white arrow). Note the foot processes of podocytes adherent to the outer surface of glomerular capillary membrane that looks markedly distorted at some sites (white arrow heads). (Uranyl acetate and lead citrate, x4000)

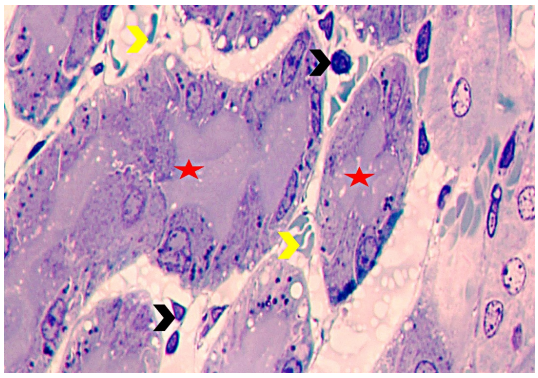

Fig. 19: A photomicrograph of a semithin section of a rat's kidney cortex from the dehydration with urografin group (group v) showing tubular lumen of proximal convoluted tubules filled with homogenous material (hyaline cast) (stars). Notice the wide interstitial space that shows red blood cells and exudate (yellow arrow head) and mononuclear cell infiltration (black arrow head). (Toluidine blue, x1000)

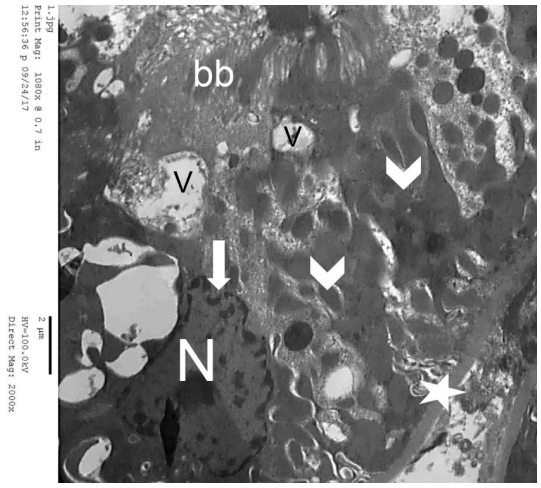

Fig. 20: An electron micrograph of an ultrathin section of a rat's renal cortex from the dehydration with urografin group (group v) showing the proximal convoluted tubule with apparent loss of the brush border (bb). The mitochondria appear amalgamated (fused) with loss of striated appearance (arrow heads). The nuclear membrane reveals numerous irregularities (arrow). Vacuolations (V), nucleus (N), epithelial basement membrane (star). (Uranyl acetate and lead citrate, x2000)

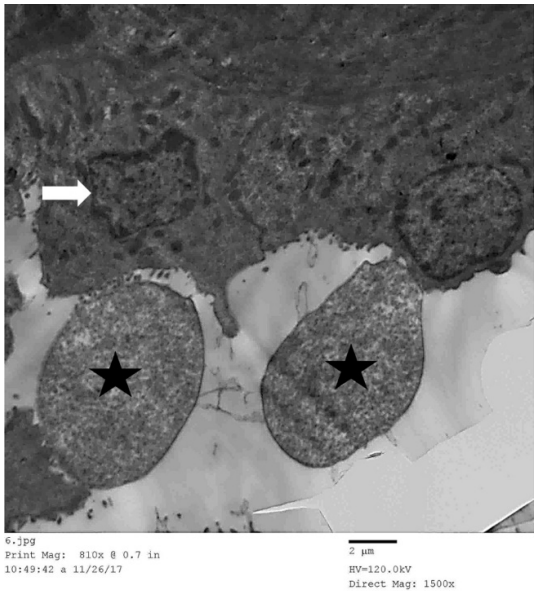

Fig. 21: An electron micrograph of an ultrathin section of a rat's kidney from the dehydration with urografin group (group v) showing the distal convoluted tubule with shrunken nucleus (white arrow), tubular lumen filled with homogenous material (stars). Notice short microvilli projecting from luminal surface of the lining epithelium. (Uranyl acetate and lead citrate, x1500)

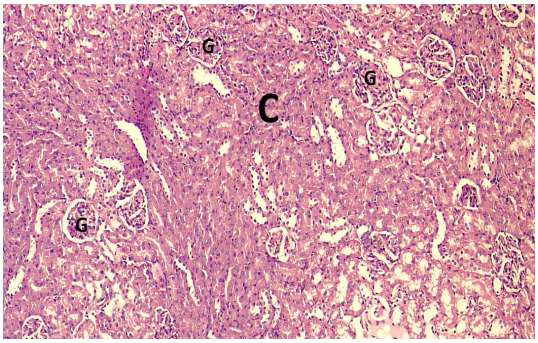

Fig. 22: A photomicrograph of a section of a rat's kidney cortex from the atorvastatin pretreatment group (group VI) showing the cortex (C) with apparently normal glomeruli (G). (H&E, x100)

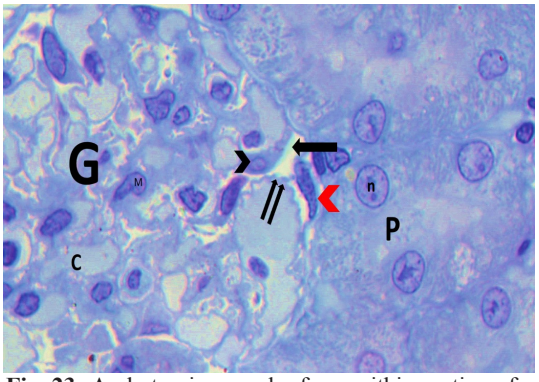

Fig. 23: A photomicrograph of a semithin section of a rat's kidney cortex from the atorvastatin pretreatment group showing a glomerulus (G) with central tufted capillaries (C), numerous irregularities of filtration membrane (double arrows), mesangial cells (M), and Bowman's space (arrow). Notice parietal layer of Bowman's capsule (red arrow head) and visceral layer (black arrow head) which surround the capillary endothelium. Notice the proximal convoluted tubules (P) which are lined by cuboidal cells with basally situated nuclei (n). (Toluidine blue, x1000)

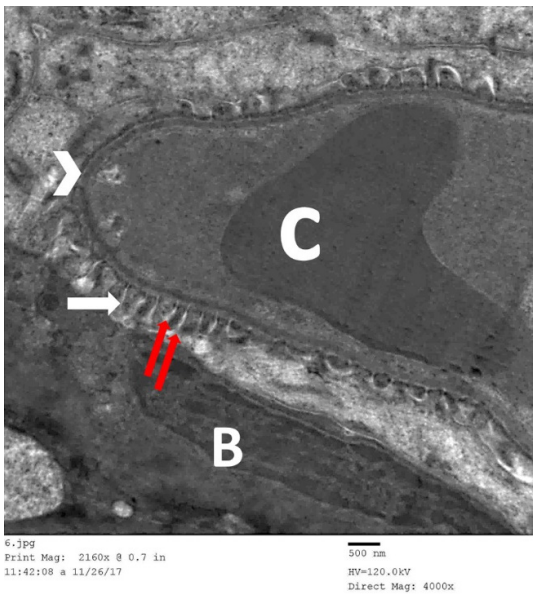

Fig. 24: An electron micrograph of an ultrathin section of atorvastatin pretreatment group of a rat's kidney cortex (group VI) showing a glomerulus capillary loop (C) with well-defined regular smooth filtration membrane of apparent normal thickness (white arrow head), foot processes (white arrow) of the podocyte are seen touching the basement membrane externally and leaving filtration slits in between (red thin arrow). Notice the parietal layer of Bowman's capsule (B) with a flat epithelial cell. (Uranyl acetate and lead citrate, x4000)

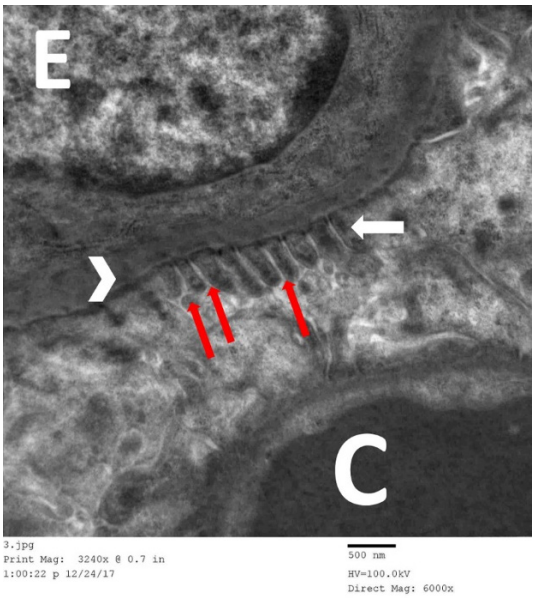

Fig. 25: An electron micrograph of an ultrathin section of atorvastatin pretreatment group of a rat's kidney cortex (group VI) showing a glomerulus capillary loop (C), well-defined regular smooth filtration membrane (white arrow head), regular smooth well defined foot process (white arrow) of the podocyte are seen touching the basement membrane externally and leaving filtration slits in between (red thin arrow). Endothelial cell (E). (Uranyl acetate and lead citrate, x6000)

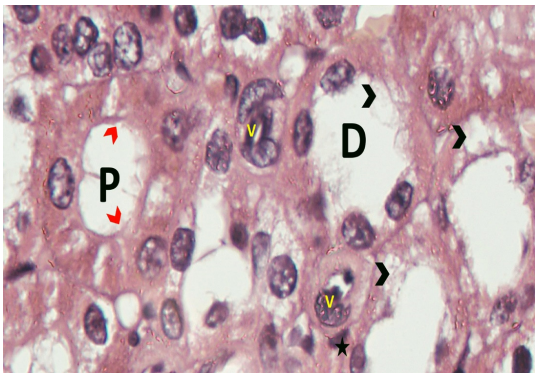

Fig. 26: A photomicrograph of a section of a rat's kidney cortex from the atorvastatin pretreatment group (group VI) showing the proximal convoluted tubule lined by cuboidal cells which shows a partial loss of brush border in some areas (red arrow heads), few vacuoles in the cytoplasm with basally situated nuclei and a narrow lumen (P). The DCT are lined by cuboidal cells with vacuolated cytoplasm (black arrow head) and have apically situated nucleus and a wide lumen (D). Note the dilated blood vessels (V) and mononuclear cell infiltration (star). (H&E, x1000)

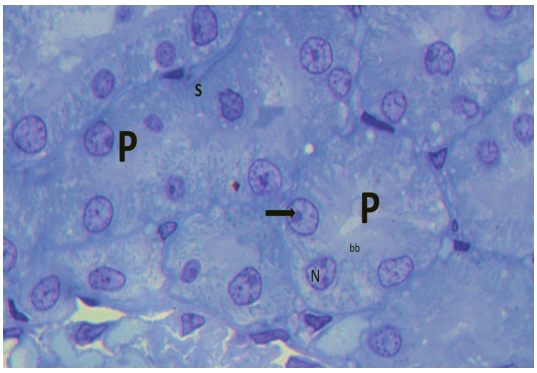

Fig. 27: A photomicrograph of a semithin section of a rat's kidney cortex from the atorvastatin pretreatment group (group VI) showing the normal structure of proximal convoluted tubules (P) which are lined by cuboidal cells with a narrow lumen, basally situated nuclei (N), prominent nucleolus (arrow), brush border (bb), and basal striations (s). (Toluidine blue, x1000)

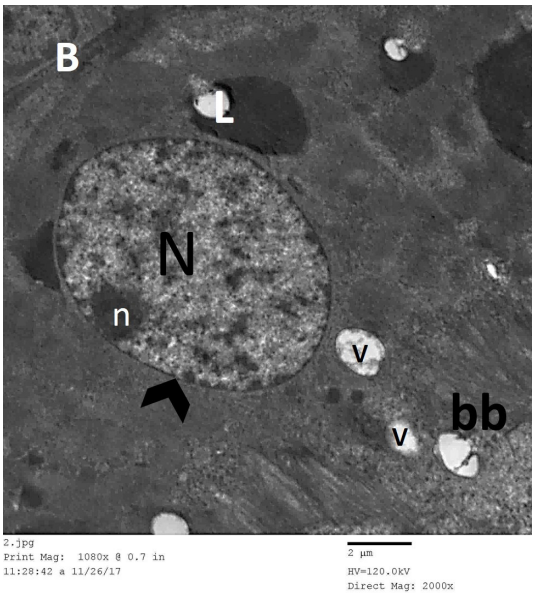

Fig. 28: An electron micrograph of an ultrathin section of a rat's kidney cortex from the atorvastatin pretreatment group (group VI) showing normal cuboidal cell lining the proximal convoluted tubule. The cell has basally situated rounded nucleus (N), prominent nucleolus (n), smooth nuclear membrane (arrow head), cytoplasm with dark dense bodies which resemble lysosomes (L), many apical vacuoles (V) and apical brush border (bb) made up of long numerous microvilli and basement membrane (B). (Uranyl acetate and lead citrate, x2000)

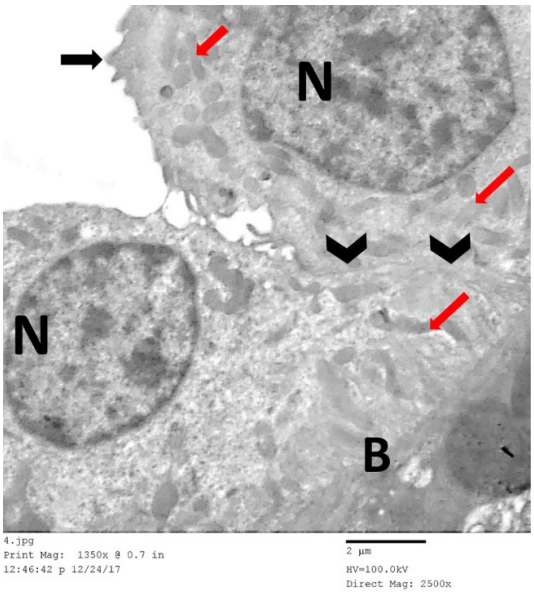

Fig. 29: An electron micrograph of an ultrathin section of a rat's kidney cortex from the statin pre-treatment group (group VI) showing the lining epithelial cells of a distal convoluted tubule with its nucleus (N), the cytoplasm shows numerous mitochondria (red arrows). The luminal border of the cell shows short sporadic microvilli (black arrow), and tight junction can be observed between adjacent lining cells (black arrow heads). (B) = basement membrane. (Uranyl acetate and lead citrate, x2500)

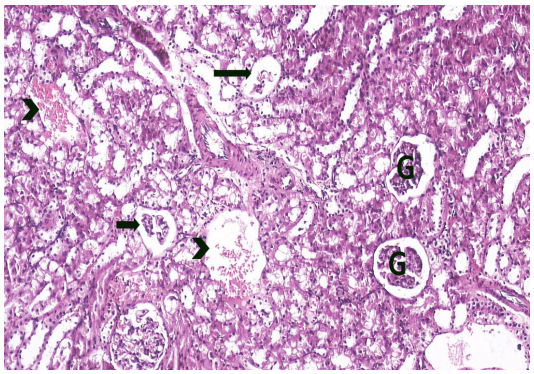

Fig. 30: A photomicrograph of a section of a rat's kidney cortex from the recovery group (group VII) showing focal shrunken and degenerated glomeruli (black arrow), normal glomeruli (G) and markedly dilated and congested blood vessels (arrow head). (H&E, x100)

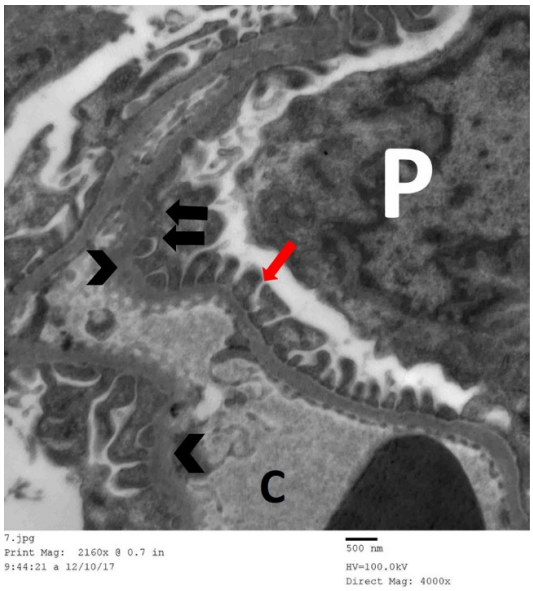

Fig. 31: An electron micrograph of an ultrathin section of a rat's kidney cortex of the recovery group (group VII) showing part of a renal corpuscle that reveals capillary lumen (C). Notice the apparent thickening of the glomerular filtration membrane at some sites (arrow heads). Note the foot processes of podocyte (P) touching the outer surface of glomerular filtration membrane (red arrow) and are distorted at some sites (black arrows). (Uranyl acetate and lead citrate, x4000)

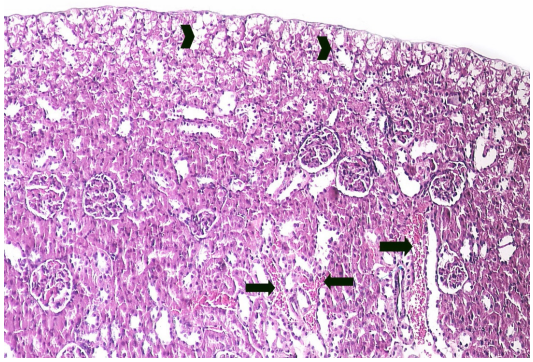

Fig. 32: A photomicrograph of a section of a rat's kidney cortex from the recovery group (group VII) showing numerous vacuolated tubules (arrow heads) in the outer cortex and multiple areas of severe vascular congestion (black arrows) in the interstitium. (H&E, x100)

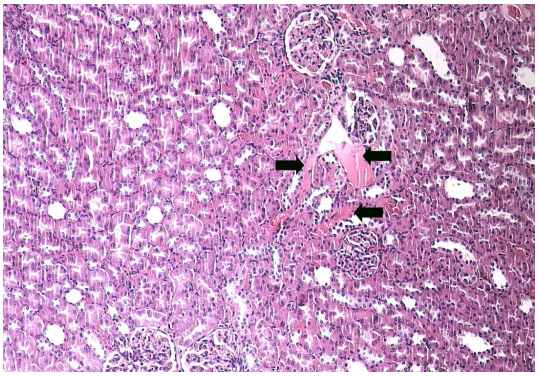

Fig. 33: A photomicrograph of a section of a rat's kidney cortex from the recovery group (group VII) showing patchy deposition of homogenous acidophilic hyaline material (black arrow) in the interstitium. (H&E, x100)

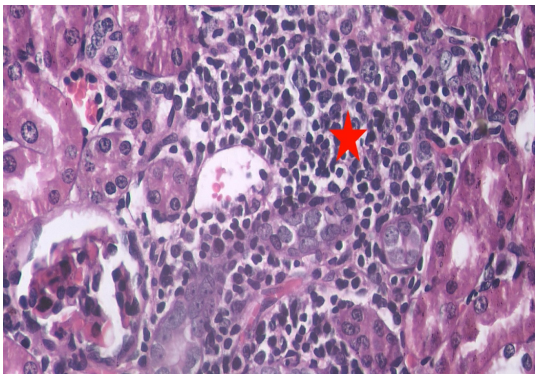

Fig. 34: A photomicrograph of a section of a rat's kidney cortex from the recovery group (group VII) showing wide patch of severe inflammatory cell infiltrate in the renal interstitium (star). (H&E, x400)

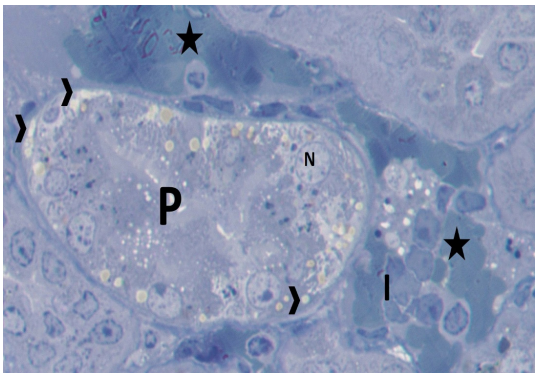

Fig. 35: A photomicrograph of a semithin section of a rat's kidney cortex from the recovery group (group VII) showing proximal convoluted tubule (P) lining cells with basal vacuolations (black arrow head). Notice the areas of hemorrhage (black stars) and inflammatory cell infiltration (I) in the peritubular region. (N) = nucleus. (Toluidine blue, x1000)

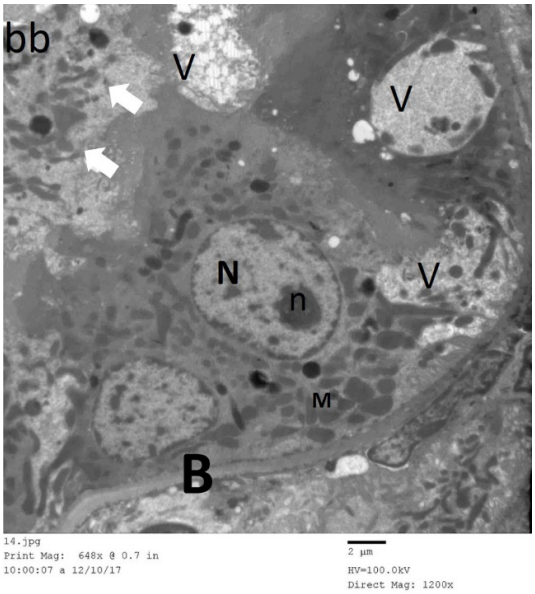

Fig. 36: An electron micrograph of an ultrathin section of a rat's kidney cortex of the recovery group (group VII) showing cuboidal cells of proximal convoluted tubule that reveals partial loss of the brush border (bb) (white arrow). The mitochondrial arrangement (M) is distorted with loss of striated appearance. Note cytoplasmic vacuolations (V) and apparently thick basement membrane (B). (N) = nucleus, (n) = nucleolus. (Uranyl acetate and lead citrate, x2000)

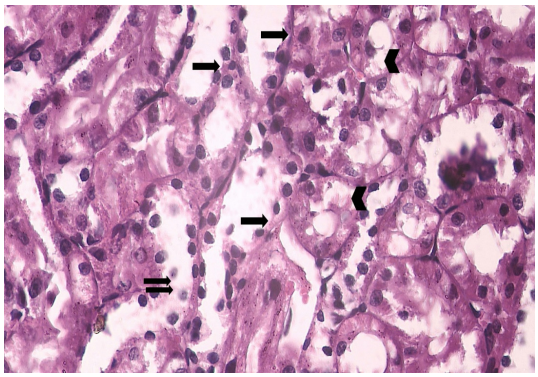

Fig. 37: A photomicrograph of a section of a rat's kidney cortex from the recovery group (group VII) showing flattening of the cells of distal convoluted tubule (black arrows), proximal convoluted tubule cell vacuolations (arrow head). Necrotic sloughed epithelial cells can be seen at some tubules (double arrows). (H&E, x1000)

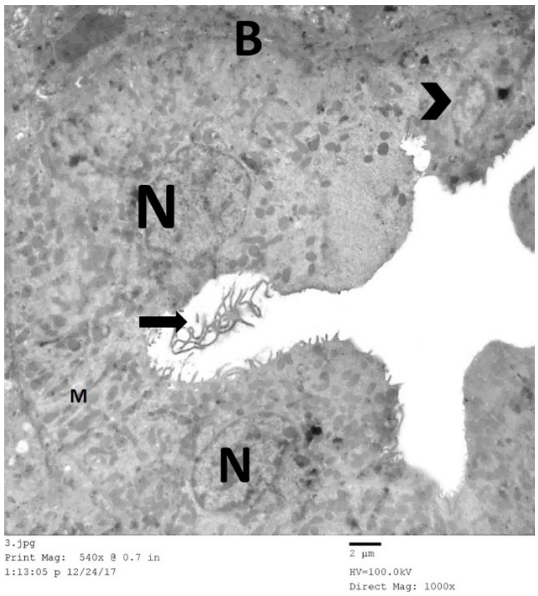

Fig. 38: An electron micrograph of an ultrathin section of a rat's kidney cortex of the recovery group (group VII) showing the distal convoluted tubule with detached microvilli into the tubular lumen (black arrow), shrunken nucleus (arrow head), mitochondria (M), nucleus (N), and basement membrane (B). (Uranyl acetate and lead citrate, x1000)

Table 1: Comparison of the mean radius of the PCT (µm) ± standard deviation (SD) between the studied groups:

Control (I)	Atorvastatin (II)	Dehydration (III)	Urografin (IV)	Dehydration with urografin (V)	Atorvastatin pretreatment (VI)	Recovery (VII)
39.95	39.102	45.42	40.11	63.74	36.96	55.68
±	±	±	±	±	±	±
2.304	2.016	1.441	1.738	3.722	3.921	8.110
	(P= 0.51)[a]	*(P< 0.0059)*[b]	*(P= 0.896)*[c]	*(P< 0.0001)*[d]	*(P= 0.138)*[a]	*(P< 0.001)*[d]
					(P< 0.0004)[e]	*(P= 0.513)*[f]

a) Non-significant decrease in comparison with control group.
b) Significant increase in comparison with control group.
c) Non-significant increase in comparison with control group.
d) Highly significant increase in comparison with control group.
e) Highly significant decrease in comparison with dehydration with urografin group.
f) Non-significant decrease in comparison with dehydration with urografin group.

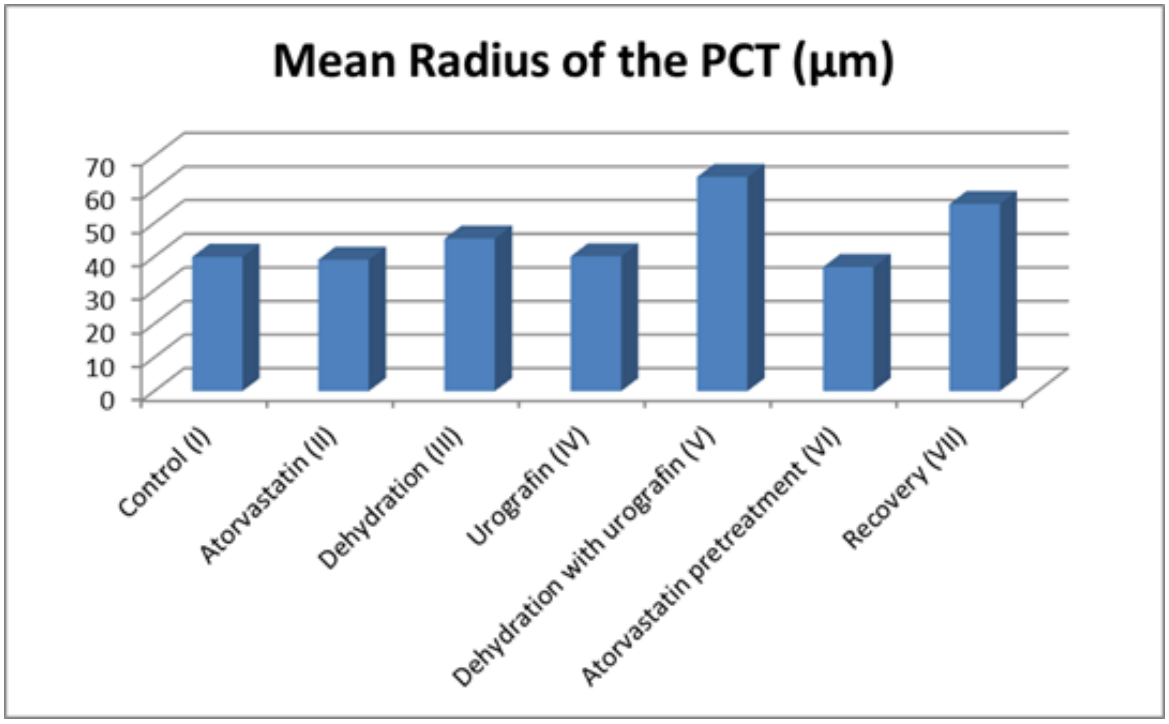

Histogram 1: Mean radius of the proximal convoluted tubules (PCT).

DISCUSSION

In this study, we aimed to show the renal damage induced by high osmolality contrast media (urografin) in the presence of dehydration as a risk factor, and to assess the possible protective role of atorvastatin on the kidney tissue.

In the present study, adult male albino rats were chosen as animal models for the experiment, being cheap, easily obtained, handled and controlled. Also, to avoid the effect of female hormones which have a role in decreasing the risk of developing kidney failure[17]. Urografin was used in the present work as the contrast agent

being popular in Egypt due to its lower economic costs. We applied dehydration as the risk factor for induction of nephropathy in rats following the model of Toprak *et al*.[12].

Examination of the renal stained sections from the atorvastatin group (group II) revealed similar results as the control group. On the other hand, examination of the renal sections from the dehydration group (group III) revealed numerous histopathological changes particularly involving the renal tubules. Glomeruli appeared hypo-cellular and shrunken. Widening of tubular lumen, necrosis and shedding of the lining tubular epithelium with tubular cast formation were observed. These findings were confirmed by the histo-morphometric study. There was a significant increase in the radius of the proximal and distal convoluted tubules, and area percentage of extravasated blood. Functional study illustrated deterioration of the renal markers of this group as a result of cell injury. There was also significant increase in serum levels of IL-6 and creatinine. However the creatinine was still within the normal range. This was in agreement with Emad *et al*.[18] who observed in histological stained sections shrunken glomeruli in the cortex, vascular congestion, tubular dilatation and tubular cast formation.

Similar results were demonstrated by Carlos *et al*.[19] in their experiment of recurrent dehydration on mice. Animals were subjected to dehydration for 5 days per week for 5 weeks. Histologically there were tubular dilatation, proximal tubular lining cell injury, and cast formation. Also, they detected the impairment of the renal function with markedly raised serum creatinine. Moreover, Ishikawa E.[20] reported a high significant increase in the BUN in rats subjected to water deprivation for 4 days. Furthermore, Lucinda[21] reported deterioration in renal function as shown by significant decline in the glomerular filtration rate (GFR) after chronic recurrent dehydration in spontaneously hypertensive rats as a model of reduced renal perfusion. Also, Leh *et al*.[22] showed that in case of reduced glomerular blood flow due to hypertension, glomerular collapse with associated glomerular atrophy occurs.

On the contrary to the results of the present study, Toprak *et al*.[12] reported that dehydration of the rats for 3 days did not reveal histopathological changes in stained renal sections with a non-significant increase in serum level of creatinine on day 6 of dehydration.

Previous researches set several explanations for the pathogenesis of renal tubular damage as a result of dehydration. Legrand *et al*.[23] reported that the necrotic changes were due to toxins and ischemia; leading to decreased renal oxygen supply, increased intracellular Ca2+ with the activation of phospholipases, proteases, and pro-apoptotic pathways leading to cell death. Miner *et al*.[24] in their clinical trial reported that dehydration activated the release of vasopressin hormone which led to vasoconstriction of blood vessels resulting in ischemic effects and cell damage with sloughing and detachment of renal necrotic cells into the tubular lumen as epithelial casts.

According to Carlos A. *et al*.[19], dehydration is associated with hyper-osmolality which activates the pathway of aldose reductase in the renal cortex. This leads to generation of fructose by the proximal tubules. The metabolism of fructose by fructokinase in the proximal tubules can lead to generation of chemokines and oxidants and that result in local tubular inflammation and subsequent injury. Vakkila and Lotze[25] reported that necrosis is accompanied by cell loss and this necrotic cell could induce local inflammation with subsequent exudate formation.

Su *et al*.[26] reported that IL-6 is a cytokine that regulates the inflammatory response, metabolism, hematopoiesis, and organ development. It is produced by tubular epithelial cells, mesangial cells, glomerular podocytes, endothelial cells, and inflammatory cells. Increase in IL-6 level has been reported to reflect several metabolic abnormalities, malignancies, as well as autoimmune and inflammatory diseases.

Dennen *et al*.[27] reported that creatinine is cleared from the blood by the kidneys, by the glomerular filtration and proximal tubular secretion. Only little tubular reabsorption of creatinine may occur. If there is impairment in the glomerular filtration, blood level of creatinine rises.

Thus, our present study proved that dehydration resulted in histopathological changes

particularly involving the glomerulus and renal tubules with significant increase in serum levels of IL-6 and creatinine, but creatinine was still within the normal range.

In the current work, light microscopic examination of the stained renal sections from rats injected with high dose of urografin (group IV) showed focal cortical histopathological affection. There was distortion of some renal corpuscles. Some tubules revealed degeneration or necrosis of their lining epithelium with the presence of tubular hyaline casts. The interstitial space demonstrated widening, hemorrhage, and marked mononuclear cell infiltrate. There was no renal function impairment for this group as proved by non-significant increase in serum creatinine and IL-6. Histo-morphometric measurements revealed non- significant increase in the radius of the proximal and distal convoluted tubules, and percent area of extravasated blood as compared with the control group.

Our current results were in agreement with the histological findings of Zhang *et al*.[28]. The authors found renal tubular necrosis and renal vascular congestion after injection of high dose of high osmolality contrast media in healthy male rabbits. However, the authors detected reduction in the renal circulation with consequent decrease in renal glomerular filtration rate by semi-quantitative analysis of a renogramcurve denoting some degree of functional affection.

Results of the current study demonstrated that injection of rats with urografin alone resulted in minor renal histological abnormalities in contrast to dehydration that led to marked structural and functional renal impairment. To our knowledge, there was scanty work on contrast media effect on healthy rats.

In the present study, light microscopic examination of stained renal sections from rats subjected to dehydration then injected with urografin dye (group V) showed severe histopathological damage of the kidney. Renal corpuscles appeared distorted with irregularities of the parietal layer of Bowman's capsule. Moreover, there were occlusion of most of Bowman's space, adherence of glomeruli with Bowman's capsule outer layer, congested glomerular capillary loop, and apparent increase in thickness of the glomerular basement membrane with hyaline material precipitation in Bowman's space. Electron microscopic examination demonstrated a thickened glomerular basement membrane and distortion foot processes of podocytes with occlusion of filtration slits at some areas.

Light microscopic examination of the convoluted tubules showed a distorted histological architecture, necrosis and shedding of the lining epithelium, and presence of hyaline casts filling the lumen. Electron microscopic examination of the convoluted tubules showed a partial loss of the brush border, mitochondrial loss of their striated appearance, and nuclear damage.

The renal interstitial spaces appeared widened, with red blood cell extravasation, inflammatory exudate, severe inflammatory cell infiltrate, and marked congested blood vessels.

Histo-morphometric measurements of this group demonstrated a highly significant increase in the radius of proximal and distal convoluted tubules, the area percentage of extravasated blood, and number of pyknotic nuclei per field in comparison to the control group (group I).

Renal function for this group showed obvious severe impairment manifested by a high significant increase in the serum level of creatinine when compared to the control group. Also, serum IL-6 recorded a highly significant increase in comparison with the control group.

These histological findings went in line with previous results[12,18,29,30]. The authors reported that a contrast agent injection in the presence of a risk factor induces a kidney structural damage. Toprak *et al*.[12] and Emad *et al*.[18] demonstrated the renal structural affection as a result of contrast media injection when associated with dehydration. Our ultrastructural findings of PCT and DCT of this group were in agreement with those reported by Emad *et al*.[18]. As regard our ultrastructural glomerular findings, they were in an agreement with those of Onk *et al*.[30] who found renal histopathological damage in diabetic rats injected with Iohexol as a contrast medium.

The functional results of the present study matched those reported before[29, 30]. Caglar *et al*.[29] reported high rise in serum levels of BUN

and creatinine. Moreover, Onk *et al*.[30] reported significant rise in the level of serum creatinine and IL-6. Our histo-morphometric results were in agreement with Onk *et al*.[30] who confirmed the cell apoptosis, necrotic changes, casts and increase in the thickness of glomerular basement membrane which were found to be higher in diabetic and contrast media groups than the control group.

Contrast medium induced nephropathy (CIN) with histopathological damage and subsequent renal function deterioration was explained by different mechanisms. Onk *et al*.[30] reported that contrast media have direct toxic effects on renal tubular cells. In addition, infusion of contrast agents increases the viscosity of blood and osmotic load resulting in renal medullary hypoxia and release of oxygen free radical; inducing post ischemic oxidative stress. Also, Goldenberg and Matetzky[31] mentioned that both oxidative stress injury and hypoxia are the main causes of CIN. Detrenis *et al*.[32] added that any decrease in the medullary blood flow with resultant hypoxia is a risk factor in the development of CIN. They added that pars recta of the distal convoluted tubules are characterized by active ion transport through their membranes with increased O2 demand. Similarly, Sarafidis *et al*.[33] reported that the proximal convoluted tubular cells are greatly affected by urografin dye due to their high oxygen consumption as they are the most metabolically active renal cells and hence they are affected by ischemia and toxins induced by the dye.

Nuclear pyknosis and cell apoptosis were noticed in the present work. O'Donnell *et al*.[34] reported that increased osmolality of contrast media induces direct renal tubular cell's DNA fragmentation. The authors examined the effect of contrast agent osmolality on dog's kidney cells in vitro. On the other side, Romano *et al*.[35] stated that contrast agents activate cell death through mitochondrial pathway by inducing marked increase in caspase-9 and caspase-3 activities with resultant fragmentation in renal tubular cells. The authors examined the effects of contrast agents on renal cell apoptosis in PCT (in porcine) and DCT (in canine).

The pathogenesis behind renal tubular cell vacuolations seen in the current study was explained by Emad *et al*.[18]. The authors stated that active entry of urografin into the renal tubular cells led to cytoplasmic vacuolations and lysosomal changes.

In the current study hyaline tubular cast were observed. Hosojima *et al*.[36] explored in their in vitro experiment on cultured PCT cells that intraluminal cast formation and albuminuria were common after urografin injection. They added that, there is a protein receptor called Megalin located in the apical brush border of the PCT and responsible for albumin uptake. The release of angiotensin decreases the expression of this protein receptors resulting in albuminuria and intraluminal cast formation.

Widening of the tubular lumen was also noted in the present work both histologically and histo-morphometrically.

Emad *et al*.[18] reported that a deposition of complexes of urinary glycoprotein-contrast in the renal tubules is the reason behind tubular dilatation.

In the present study, renal interstitium was widened and revealed vascular congestion and extravasation. Miner *et al*.[24] believed that accumulation of toxins caused by the dehydration of rats was the cause of damage and erosion of blood vessels with resultant hemorrhage. Also, Sutton[37] added that the increased microvascular permeability leads to the trapping of red blood cells into the interstitial space.

Thus, our present work proved that administration of urografin in presence of dehydration as a precipitating factor resulted in histopathological changes particularly involving the glomeruli and renal tubules with highly significant increase in serum levels of creatinine and IL-6.

In the present work, pretreatment of the rats with high dose atorvastatin for 5 days ameliorated the severe structural changes of the kidney and restored the renal function in comparison with the dehydration with urografin group (group V). Reviewing the literature, there were few reported studies on the preventive role of atorvastatin against urografin (high osmolality contrast media) induced nephropathy.

Examination of stained renal sections of rats from atorvastatin pretreatment group (group VI) showed less tubular damage with less vacuolated tubular cells, partially intact brush border of proximal convoluted tubules, and marked reduction in tubular casts. This was in agreement with Su *et al*.[11] who assessed the effect of atorvastatin on iopromide (low osmolar contrast agent) induced nephropathy on diabetic rats. They reported that high dose atorvastatin ameliorated the presence of tubular vacuolar degeneration, hyaline and cellular casts, renal tubular cell apoptosis, and infiltration with inflammatory cells. Moreover, in an animal study, Ketab *et al*.[38] used adult rats dehydrated for 24 hours and administered oral simvastatin daily for 4 days, then the contrast media iohexol was infused, and all rats were sacrificed on day 5. The authors reported that simvastatin was found to attenuate contrast-induced nephropathy effects with minimal tubular pathology.

Nearly normal histological findings in this group were confirmed by the morphometric study. In the current study, there was a highly significant decrease in the radius of both proximal and distal convoluted tubules, the area percentage of extravasated blood, and the number of pyknotic nuclei per field in comparison to dehydration with urografin group (group V). This was in agreement with Su *et al*.[11] who investigated in their experiment the effect of pretreatment of diabetic rats with rising doses of atorvastatin (5, 10, 30 mg/kg) in preventing iopromide induced nephropathy. They reported that moderate and high dose atorvastatin resulted in no inflammatory reaction.

In the present study there was highly significant decrease in the thickness of glomerular basement membrane in atorvastatin pretreatment group (group VI) when compared to dehydration with urografin group (group V). This was in agreement with Connell *et al*.[39] who recorded that statin improves the indices of podocyte foot-process base width and thickness of glomerular basement membrane on transmission electron microscopy. Also, Vázquez-Pérez *et al*.[40] reported that atorvastatin prevented the dysfunction of renal artery endothelium, glomerular basement membrane thickening, and glomerular hypertrophy in hyper-cholesterolaemic rabbits.

Results of present study revealed a highly significant decrease in the serum levels of IL-6 and creatinine in the atorvastatin pretreatment group in comparison to the dehydration with urografin group (group V). Su *et al*.[11] recorded that the serum creatinine was lower in low, moderate, and high dose atorvastatin pretreated groups as compared with the diabetes mellitus and contrast media (iopromide) group. Moreover, Ketab *et al*.[38] assessed the effect of oral simvastatin daily for 4 days, followed by dehydration of adult rats for 24 hours, then administration of contrast media iohexol, and animals were sacrificed on the 5th day. The authors reported a significant decrease in blood urea nitrogen and serum creatinine levels in the experimental animals. Also, Deng *et al*.[41] added that treatment with oral rosuvastatin at a dose of 10 mg/kg/day (moderate dose) for 5 days has significantly reduced the increase in serum creatinine and IL-6 caused by contrast media (high-osmolar contrast medium meglumine amidotrizoate).

Also, in a met-analysis of 21 randomized control trials in patients prepared for coronary angiography/ percutaneous coronary intervention, it was found that both atorvastatin and rosuvastatin were the most beneficial in guarding against CIN. However, the effect of simvastatin in prevention of CIN, and whether the high dose statin is better than the lower doses were not clear[42].

As mentioned before, the renal cellular structural damage induced by dehydration with contrast media was partially mediated by reducing the renal blood flow with resulting ischemia, hypoxia and oxidative stress with release of oxygen free radicals[31].

In the present study, atorvastatin pretreatment reversed the renal pathology as seen in (group VI). This was mediated in part by improving renal perfusion as mentioned by previous researchers[43-45].

According to Bonetti *et al*.[43], statins can decrease endothelin synthesis and down-regulate angiotensin receptors preventing renal hypo-perfusion and ischemia. Bao *et al*.[44] and Babelova *et al*.[45] added that statins increase nitric oxide level leading to reduction in platelet aggregation, enhancing cell proliferation as well as improved microcirculation.

Deng *et al*.[41] reported that rosuvastatin treatment ameliorated the inflammatory response and cell death, and suppressed the oxidative stress in a diabetic rat using meglumine amidotrizoate, a high-osmolar contrast medium. Another mechanism for renal toxicity in CIN was the direct effect on renal cells[30]. Stimulation of both caspase-3 and caspase-9 activities with resultant apoptosis was also reported[35]. Moreover, Haylor *et al*.[46] recorded that atorvastatin has an inhibitory effect on caspase-3 enzyme preventing cell apoptosis. In addition, Mizuguchi *et al*.[47] proved that atorvastatin decreases renal tubular cell death and interstitial fibrosis through inhibition of expression of the transforming growth factor beta by tubular cells.

Moreover, statins help renal tissue regeneration through their ability to enhance cell proliferation[44].

In the present study nephrotoxicity due to contrast media and dehydration was associated with inflammatory reaction as evident histologically and by raised serum IL-6 level. These features were inhibited by atorvastatin pretreatment as explained before[41, 45]. Babelova *et al*.[45] stated that statins have anti-inflammatory effects. It reduces T cell activation with reduction of cytokine release and hence decreases circulating inflammatory biomarkers.

In addition, statins have many other mechanisms of action that may favor protection of the renal tissue against CIN like modulation of thrombosis and coagulation and induction of neovascularization in ischemic tissue[45].

A clinical study was conducted by Patti *et al*.[48] showed that high dose atorvastatin pretreatment for short period was effective protective factor against contrast- induced nephropathy in patients with acute coronary diseases undergoing percutaneous coronary intervention. Furthermore, Marenzi *et al*.[49] reported in their meta-analysis of nine randomized control trials comparing the use of short term pre-procedural high dose statin to the control group. It showed that there was a 50 % reduction in CIN for high dose pre-procedural statin treatment in comparison to the control group. Also, Yang *et al*. (50) mentioned in their meta-analysis that the patients who received rousovastatin before cardiac catheterization were found to have 51% lower risk of CIN in comparison with the control group. However, rosuvastatin treatment was not effective in prevention of CIN in patients undergoing elective coronary catheterization.

In the current work, the recovery group (group VII) in which rats were subjected to high dose urografin and left for 2 weeks showed shrunken, degenerated, glomeruli with markedly dilated congested blood vessels in the interstitium. Apparent thickening of glomerular capillary basement membrane with distorted and fused foot processes at some sites were also noticed. Other areas revealed accumulation of large number of inflammatory cell infiltrate. PCT showed nuclear membrane irregularity, partial loss of the brush border, and little number of mitochondria that appeared distorted with lost striated appearance. Also, there were numerous vacuolations occupying the basal and apical parts of the cytoplasm. DCT revealed flattening of the lining epithelial cells, cytoplasmic vacuolations, sloughed cells at some tubules, detached brush border microvilli, shrunken nuclei, and loss of histological architecture of cytoplasmic organelles.

On comparing the recovery group (group VII) with the dehydration with urografin group (group V), there was a non-significant decrease in the radius of both proximal and distal convoluted tubules. On the other hand, there was a significant decrease in area percentage of extravasated blood, number of pyknotic nuclei per field, and thickness of the glomerular basement membrane. Also, there was a significant decrease in serum IL-6 and creatinine on comparing the recovery group (group VII) with the dehydration with urografin group (group V).

In the present study, on comparing the recovery group (group VII) with the control group (group I), there was a significant increase in the radius of both proximal and distal convoluted tubules, area percentage of extravasated blood, number of pyknotic nuclei per field, and thickness of the glomerular basement membrane. Also, there was a high significant increase in serum creatinine, and a significant increase in serum level of IL-6. These findings revealed that there was still some degree of kidney dysfunction which did not improve completely after 2 weeks.

This was in agreement with Hopkinson *et al*.[51] who conducted a cohort study on diabetic patients undergoing coronary angiography and evaluated the link between diabetes as a precipitating factor for CIN and the long-term outcomes of CIN including renal dysfunction at 3 months, the need for dialysis, and mortality. The study reported cases with end-stage kidney disease which indicate permanent dialysis with an increase in mortality rate. Also, Sigterman *et al*.[52] reported that exposure to iodinated contrast media during endovascular interventions for peripheral arterial disease results in CIN with increasing the incidence of long-term kidney impairment and cardiovascular insults with death.

Moreover, Maioli *et al*.[53] reported that CIN is a temporary process, and kidney function returns to normal within one-two weeks of contrast administration. Unfortunately, less than one-third of patients developed renal impairment less than 1% of patients needed dialysis. The incidence is higher in patients having underlying renal problems. The bad news is 18% of the CIN patients who need dialysis will require it permanently.

CONCLUSIONS

It was concluded that the use of high osmolality contrast media (urografin) in presence of dehydration as a risk factor in the adult male albino rat caused manifest structural changes in the renal tissues affecting the glomeruli, renal tubules, and affecting also the renal function. All these effects were improved by administration of high dose atorvastatin for 5 consecutive days prior to urografin injection. During recovery without administration of atorvastatin, some features of the renal damage remained indicating the failure of complete recovery.

CONFLICT OF INTERESTS

There are no conflicts of interest.

REFERENCES

1. Pannu N, Wiebe N, and Tonelli M. Prophylaxis strategies for contrast-induced nephropathy. JAMA. 2006; 295(23):2765-2779.

2. Zhang J, Ying Gao X, and Zheng Y. Efficacy of alprostadil for preventing of contrast-induced nephropathy: A meta-analysis. Nature scientific reports. 2017; 7:1045-1049.

3. Stacul F, van der Molen A, and Reimer P. Contrast induced nephropathy: ESUR Contrast Media Safety Committee guidelines. 2011; 21:2527–2541.

4. Seeliger E, Sendeski M, and Rihal C. Contrast-induced kidney injury: mechanisms, risk factors, and prevention European Heart Journal. 2012; 33(1):2007–2015.

5. Tumlin J, Stacul F, and Adam A. Pathophysiology of contrastinduced nephropathy. Am J Cardiol. 2006; 98:14K–20K.

6. Sendeski MM. The pathophysiology of renal tissue damage by iodinated contrast media, Clin Exp Pharmacol Physiol. 2011; (38):292-299.

7. Rosenstock JL, Bruno R, and Kim JK. The effect of withdrawal of ACE inhibitors or angiotensin receptor blockers prior to coronary angiography on the incidence of contrast-induced nephropathy. Int Urol Nephrol. 2008; 40:749–755.

8. Mruk B. Renal Safety of Iodinated Contrast Media Depending on Their Osmolality - Current Outlooks. Pol J Radiol. 2016; 81:157-65.

9. Taylor FC, Huffman M, and Ebrahim S. Statin therapy for primary prevention of cardiovascular disease. JAMA. 2013; 310(22): 2451–2.

10. Buemi M, Senatore M, and Corica F. Statins and progressive renal disease. Med Res Rev. 2002; 22:76–84.

11. Su J, Zou W, and Cai W. Atorvastatin ameliorates contrast medium-induced renal tubular cell apoptosis in diabetic rats via suppression of Rho-kinase pathway. European Journal of Pharmacology. 2014; 723:15–22.

12. Toprak O, Cirit M, and Tanrisev M. Preventive effect of nebivolol on contrast-

induced nephropathy in rats. Nephrol Dial Transplant. 2008; 23:853–859.

13. Gaber M, Hussein A, and Sherif I. Renal ischemia / reperfusion injury in type II DM: possible role of proinflammatory cytokines, apoptosis, and nitric oxide. Journal of physiology and pathophysiology. 2011; 2(1): 6-17.

14. Graham L and Orenstein JM. Processing tissue and cells for transmission electron microscopy in diagnostic pathology and research. Nature Protocols. 2007; 2(10): 2439-2450.

15. Drury RAB and Wallington EA. Carleton's histological technique fifth edition oxford university press, New York. 1980; p: 520.

16. Bancroft J and Gamble M. Bancroft's theory and practice of histological techniques, 7th edition, Elsevier, London. 2013; pp. 69-95.

17. Seppi T, Prajczer S, and Dörler MM. Sex Differences in Renal Proximal Tubular Cell Homeostasis. J Am Soc Nephrol. 2016; (10):3051-3062.

18. Emad M, El-Sherif M, and Abd-El Wahed M. Effect of urografin on the Kidney of Adult Female Albino Rat and the Possible Protective Role of Nebivolol: A Morphological and Ultrastructural Study. Life Science Journal. 2013; 10(4): 248-261.

19. Carlos A, Takuji I, and Miguel A. Fructokinase activity mediates dehydration induced renal injury. Kidney international. 2013; 86:294-302.

20. Ishikawa E. Experimental study of effect of water deprivation-induced dehydration on renal function in rats. Hinyokika Kiyo. 1987; 33(9):1342-8.

21. Lucinda M, Katrina M, and Louise L. Chronic recurrent dehydration associated with periodic water intake exacerbates hypertension and promotes renal damage in male spontaneously hypertensive rats. Scientific Reports. 2016; 6:33855.

22. Leh S, Hultström M, and Rosenberger C. Afferent arteriolopathy and glomerular collapse but not segmental sclerosis induces tubular atrophy in old spontaneously hypertensive rats. Virchows Archiv. 2011; 459(1): 99–108.

23. Legrand M, Mik EG, Johannes T. Renal Hypoxia and Dysoxia After Reperfusion of the Ischemic Kidney. Molecular Medicine. 2008; 14:502–516.

24. Miner S, Dzavik V, and Nguyen P. N-Acetylcysteine reduces contrast-associated nephropathy but not clinical events during long term follow-up. American Heart Journal.2004; 148:690–695.

25. Vakkila J and Lotze M. Inflammation and necrosis promote tumor growth. Nature Reviews Immunology. 2004; 4:641–648.

26. Su H, Lei Ch, and Zhang Ch. Interleukin-6 Signaling Pathway and Its Role in Kidney Disease: An Update. Front Immunol. 2017; 8:405-415.

27. Dennen P, Altmann CH, and Kaufman J. Urine interleukin-6 is an early biomarker of acute kidney injury in children undergoing cardiac surgery. Crit Care. 2010; 14(5): R181.

28. Zhang Y, Wang J, and Zhang J. Effect of Iodinated Contrast Media on Renal Function Evaluated with Dynamic Three-dimensional MR Renography. Radiology. 2014; 270:409-415.

29. Caglar Y, Mete UO, and Kaya M. Ultrastructural evaluation of the effects of the contrast media on the rat kidney. Journal of Submicroscopic Cytology and Pathology. 2001; 33:443- 451.

30. Onk D, Onk O, and Turkmen K. Melatonin Attenuates Contrast-Induced Nephropathy in Diabetic Rats: The Role of Interleukin-33 and Oxidative Stress. Mediators of Inflammation. 2016; 1-10.

31. Goldenberg I and Matetzky S. Nephropathy induced by contrast media: pathogenesis, risk factors and preventive strategies.

Canadian Medical Association Journal. 2005; 172(11):1461–1471.

32. Detrenis S, Meschi M, and Musini S. Lights and shadows on the pathogenesis of contrast-induced nephropathy: state of the art. Nephrol Dial Transplant. 2005; 20:1542–1550.

33. Sarafidis P, Whaley- Connell A, and Sowers J. Cardiometabolic syndrome and chronic kidney disease: what is the link? Journal of the Cardiometabolic Syndrome. 2006; 1(1): 58–65.

34. O'Donnell DH, Moloney MA, and Bouchier-Hayes DJ. Contrast-Induced Nephrotoxicity, Possible Synergistic Effect of Stress Hyperglycemia. American Journal of Roentgenology. 2010; 195:45–49.

35. Romano G, Briguori C, and Quintavalle C. Contrast agents and renal cell apoptosis. Eur Heart J. 2008; 29:2569–2576.

36. Hosojima M, Sato H, and Yamamoto K. Regulation of megalin expression in cultured proximal tubule cells by angiotensin II type 1A receptor- and insulin-mediated signaling cross talk. Endocrinology. 2009; 150:871–878.

37. Sutton TA. Alteration of microvascular permeability in acute kidney injury. Microvascular Research. 2009; 77:4–7.

38. Ketab E, Abdulrahman M, and Tariq M. Simvastatin Attenuates Contrast-Induced Nephropathy through Modulation of Oxidative Stress, Proinflammatory Myeloperoxidase, and Nitric Oxide. Oxidative Medicine and Cellular Longevity. 2012; 1-8.

39. Connell A, Habibi J, and Nistala R. Attenuation of NADPH Oxidase Activation and Glomerular Filtration Barrier Remodeling with Statin Treatment. Hypertension. 2008; 51(2):474-480.

40. Vázquez-Pérez S, Aragoncillo P, and de Las Heras N. Atorvastatin prevents glomerulosclerosis and renal endothelial dysfunction in hypercholesterolaemic rabbits. Nephrol Dial Transplant. 2001; 16:40–44.

41. Deng J, Wu G, and Yang CH. Rosuvastatin attenuates contrast-induced nephropathy through modulation of nitric oxide, inflammatory responses, oxidative stress and apoptosis in diabetic male rats. Journal of Translational Medicine. 2015; (13):13-53.

42. Haixia Li, Wang C, and Liu C. Efficacy of Short Term Statin Treatment for the Prevention of Contrast-Induced Acute Kidney Injury in Patients Undergoing Coronary Angiography/ Percutaneous Coronary Intervention: A Meta-Analysis of 21 Randomized Controlled Trials. Am J Cardiovasc Drugs. 2016; 16:201–219.

43. Bonetti PO, Lerman LO, and Napoli C. Statin effects beyond lipid lowering—are they clinically relevant? Eur Heart J. 2003; 24:225–48.

44. Bao N, Minatoguchi S, and Kobayashi H. Pravastatin reduces myocardial infarct size via increasing protein kinase C-dependent nitric oxide, decreasing oxyradicals and opening the mitochondrial adenosine triphosphate-sensitive potassium channels in rabbits. Circulation Journal. 2007; 71(10):1622–1628.

45. Babelova A, Sedding DG, and Brandes RP. Antiatherosclerotic mechanisms of statin therapy. Curr Opin Pharmacol. 2013; 13:1-5.

46. Haylor JL, Harris KP, and Nicholoson M L. Atorvastatin improving renal ischemic reperfusion injury via direct inhibition of active caspase-3 in rats. Exp Biol Med (Maywood). 2011; 236:755-763.

47. Mizuguchi Y, Miyajima A, and Kosaka T. Atorvastatin ameliorates renal tissue damage on unilateral ureteral obstruction. J Urol. 2004; 172:2456-2459.

48. Patti G, Ricottini E, and Nusca A. Short-Term, High-Dose Atorvastatin Pretreatment to Prevent Contrast-Induced Nephropathy in Patients With Acute Coronary Syndromes Undergoing Percutaneous Coronary Intervention (from the ARMYDA-CIN [Atorvastatin for Reduction of Myocardial Damage during Angioplasty Contrast-Induced Nephropathy] Am J Cardiol. 2011; 108(1):1-7.

49. Marenzi G, Cosentino N, and Werba JP. A meta-analysis of randomized controlled trials on statins for the prevention of contrast-induced acute kidney injury in patients with and without acute coronary syndromes. Int J Cardiol. 2015; 183:47–53.

50. Yang Y, Yan-xian Wu, and Hu Yz. Rosuvastatin Treatment for Preventing Contrast-Induced Acute Kidney Injury after Cardiac Catheterization. A Meta-Analysis of Randomized Controlled Trials. Medicine. 2015; 94(30):e1226.

51. Hopkinson DA, Powell SP, and Chawla. Abstract 370: Outcomes in Patients with Diabetes Undergoing Coronary and Peripheral Angiography and Intervention. Arteriosclerosis, Thrombosis, and Vascular Biology. 2017; 1(37): A370.

52. Maioli M, Toso A, and Leoncini M. Persistent renal damage after contrast-induced acute kidney injury: incidence, evolution, risk factors, and prognosis. Circulation. 2012; 125(25):3099-3107.

53. Sigterman TA, Krasznai AG, and Snoeijs MG. Contrast Induced Nephropathy and Long-term Renal Decline after Percutaneous Transluminal Angioplasty for Symptomatic Peripheral Arterial Disease. European Journal of Vascular and Endovascular Surgery. 2016; 51(3):386-393.

عقار أتورفاستاتين يخفف من اعتلال الكلى الناجم عن صبغة يوروجرافين في وجود الجفاف كعامل خطورة: دراسة هستولوجية وقياسية على نموذج الفأر

أمل حاسم محمد فؤاد[١]، محب فريد منير رفله[١]، هدى محمد محمود[١]، نجوى ابراهيم النفياوى[١]، يوسف شكري عبد العال[١]، أحمد فريد النكلاوي[٢،١]

١. قسم التشريح والأجنة، كلية الطب، جامعة عين شمس، مصر.

٢. قسم علوم وظائف الأعضاء، كلية فقيه للعلوم الطبية، جدة، المملكة العربية السعودية.

ملخص البحث

في هذه الدراسة ، تم تقييم الدور الوقائي لعقار أتورفاستاتين على إصابة الكلى الناجمة عن صبغة يوروجرافين مع وجود الجفاف كعامل خطورة. تم تقسيم اثنين واربعين من ذكور الفئران البيضاء البالغة عشوائيًا إلى سبع مجموعات (٦ فئران / مجموعة). المجموعة الأولى (المجموعة الضابطة) ، المجموعة الثانية (مجموعة أتورفاستاتين) ، المجموعة الثالثة (مجموعة الجفاف) ، المجموعة الرابعة (مجموعة صبغة يوروجرافين)، المجموعة الخامسة (مجموعة الجفاف مع صبغة يوروجرافين) ، المجموعة السادسة (المجموعة المعالجة بعقار أتورفاستاتين) ، والمجموعة السابعة (مجموعة الانتعاش). في نهاية التجربة لكل مجموعة ، تم الحصول على عينات دم لتقدير مستويات مصل الدم من الكرياتينين وinterleukin-6. بعد التضحية ، تم استخراج الكلى وإعدادها للفحص بالمجهر الضوئي والمجهر الإلكتروني النافذ. أظهر فحص شرائح الكلى من كل من المجموعة الثالثة والمجموعة الرابعة زيادة واضحة في نصف قطر الأنيبيبات الملتوية القريبة والبعيدة. كما شوهد الهيالين المصبوب ، وخلايا أنبوبية مفرغة ، واحتقان للأوعية الدموية. علاوة على ذلك ، كانت هناك زيادة في مستويات مصل الدم لكل من interleukin-6 والكرياتينين. لوحظت كل هذه النتائج في المجموعة الخامسة أيضًا. وبالإضافة إلى ذلك ، كانت هناك زيادة واضحة في عدد الأنوية الداكنة. كانت هناك زيادة في سمك الغشاء القاعدي الكبيبي وعدم انتظام في زوائد الخلايا القدمية. تم تحسين كل هذه التغييرات باستخدام عقار أتورفاستاتين في المجموعة السادسة. أما في المجموعة السابعة ، فقد لوحظت بعض ملامح الضرر الكلوي مما يشير إلى فشل الشفاء التام. ولقد أكدت النتائج القياسية والتحليل الإحصائي النتائج النسيجية. وقد استنتج من هذه الدراسة أن عقار أتورفاستاتين يحمي الكلى من الإصابة الناجمة عن صبغة يوروجرافين في وجود الجفاف كعامل خطورة.